



INFLUENCE OF SILICA FUME ON THE WORKABILITY AND THE COMPRESSIVE STRENGTH OF HIGH-PERFORMANCE CONCRETES

R. Duval¹ and E.H. Kadri

Laboratoire de Matériaux et Science des Constructions, Université de Cergy-Pontoise,
Rue d'Eragny, Neuville-sur Oise, 95031 Cergy-Pontoise Cedex, France

(Received June 25, 1997; in final form January 8, 1998)

ABSTRACT

The workability and the compressive strength of silica fume concretes were investigated at low water-cementitious materials ratios with a naphthalene sulphonate superplasticizer. The results show that partial cement replacement up to 10% silica fume does not reduce the concrete workability. Moreover, the superplasticizer dosage depends on the cement characteristics (C_3A and alkali sulfates content). At low water-cementitious materials ratios, slump loss with time is observed and increases with high replacement levels. Silica fume at replacement contents up to 20% produce higher compressive strengths than control concretes; nevertheless, the strength gain is less than 15%. In this paper, we propose a model to evaluate the compressive strength of silica fume concrete at any time. The model is related to the water-cementitious materials and silica-cement ratios. Taking into account the author's and other researchers' experimental data, the accuracy of the proposed model is better than 5%.
© 1998 Elsevier Science Ltd

Introduction

The use of silica fume in combination with a superplasticizer is now a usual way to obtain high-strength concretes. The improvement of mechanical properties of concretes with silica fume accounts for the increasing consumption of this admixture in concrete. Furthermore, apart from mechanical properties, the durability of high-performance concretes concerning the most common harmful ions (sulfate, chloride, seawater) is also improved; indeed the reduction of permeability that is due to the more compact microstructure of concrete slows down the diffusion of ions. Nevertheless, various authors point out some drawbacks regarding the use of silica fume in concretes. Among these, the loss of plasticity during the production of concrete and the great sensitivity to plastic shrinkage during the initial curing are the most important. However researchers seem to disagree about the interpretation of the exact role silica fume plays in the increase of mechanical strengths.

Some authors claim that silica fume improves the strength of the bond between the aggregates and the cement matrix (1–5). The partial replacement of cement by silica fume

¹To whom correspondence should be addressed.

increases the strength of mortar and concrete; yet it does not seem to have an important impact on the strength of pure cement paste. To other researchers, however, the positive result due to the admixture of silica fume stems from the increase in strength of the cement matrix (6,7). Researchers also disagree about the definition of the optimal content of silica fume, which enables us to obtain the highest strengths. To some researchers (8,9), the content is about 15%, whereas to others (5,10), the increase in compressive strength may reach from 30 to 40% of replacement of cement by silica fume.

In this study, we aim at defining the influence of the content of silica fume on the workability and the compressive strength of concrete. Moreover, we introduce a prediction model of the compressive strength of concrete depending on time.

Experimental Procedure

Basic Materials

We used two crushed limestone aggregates from the “Boulonnais” region with a granular size of 5–12.5 mm and 12.5–20 mm.

The compressive strength of the aggregates varies from 140 to 180 MPa. Their saturated surface dried (SSD) specific gravity was 2.70 and the absorption of 0.5%. The fine aggregate is composed of a mixture of 50% of rolled sand from the “Seine” region and 50% of crushed sand from the “Boulonnais” region. The sand has a specific gravity of 2.65, an absorption of 0.80%, and a fineness modulus of 2.56.

The physical properties and chemical analyses of cements C1, C2, and silica fume are given in Table 1. Both cements, whose specific area is about 400 m²/kg, have an identical content of tricalcium silicate, yet they have a different content of tricalcium aluminate. The C2 cement, which may be used in seawater and in a sulphate water environment, has a low percentage of C₃A (2%), whereas the C1 cement has a normal C₃A content (10%). Natural gypsum is added as a setting regulator in the two cements. The SO₃ content of alkali sulfates was, respectively, 0.65% and 0.45% in the clinkers from which the cements C1 and C2 were made.

The silica fume contains 89% of SiO₂ with a density of 2.1 and a bulk density of 600 kg/m³; its BET specific area is 18.2 m²/g. The superplasticizer we used is a naphthalene sulphonate condensate with 40% solids content that has a specific gravity of 1.21.

In order to get homogeneous samples, we adapted the content of superplasticizer so that the slump remains constant. The slump is about 170 to 200 mm to get a fluid consistency of concrete.

Test Details

The mixing parameters for the high strength concretes with the two Portland cements are presented in Table 2. The mixing procedure to get the concrete samples was as follows:

1. The dry aggregates and the cementitious materials (cement and silica fume) were mixed without water for 1 min.
2. Mixing water was added with one third of the volume of superplasticizer, then the mixing was continued for 2.5 min.

TABLE 1
Physical properties and chemical analyses of cements C1, C2, and silica fume.

Description of tests	Portland Cement (CPA CEM 52.5) “C1”	Portland Cement (CPA CEM 52.5 PM CP2) “C2”	Silica fume
Physical tests: Time of set (Vicat)			
initial	2 h 35 min.	2 h 50 min.	—
final	4 h 55 min.	5 h 20 min.	—
Surface area (Blaine)	395 m ² /kg	390 m ² /kg	—
Mortar strength			
Compressive strength at:			
2-days	35 MPa	30 MPa	—
7-days	50 MPa	44 MPa	—
28-days	62 MPa	60 MPa	—
Chemical analysis			
Silicon dioxide (SiO ₂)	19.8%	21.2%	89%
Aluminum oxide (Al ₂ O ₃)	5.14%	3.2%	0.3%
Ferric oxide (Fe ₂ O ₃)	2.3%	3.9%	0.6%
Calcium oxide (CaO), total	64.9%	65.7%	0.3%
Magnesium oxide (MgO)	0.9%	1.5%	1.1%
Sulphur trioxide (SO ₃), total	3.4%	2.1%	0.2%
Potassium oxide (K ₂ O)	1.1%	0.4%	1.6%
Sodium oxide (Na ₂ O)	0.05%	0.1%	0.6%
Silicium (Si)	—	—	3.2%
Loss on ignition	1.1%	1.2%	2.7%
Insoluble residue	0.2%	0.05%	—
Compound composition			
Tricalcium silicate (C ₃ S)	58%	59%	
Dicalcium silicate (C ₂ S)	13%	16%	
Tricalcium aluminate (C ₃ A)	10%	2%	
Tetracalcium aluminoferrite (C ₄ AF)	7%	12%	

3. The remaining superplasticizer was added with a last 1-min. mixing.

The addition of silica fume was obtained by replacing part of the cement with the same weight of silica fume. The silica fume content was 0, 10, 20, 30% of the cement weight for all mixtures. Four binder dosages (cement + silica fume) were experimented: 550, 460, 400, and 310 kg/m³.

The superplasticizer was added as a weight percentage in relation to the binder and the dosage was determined thanks to the “grout method” (11). This superplasticizer has a good compatibility with the two cements and was used in several structures made of high strength concrete. The total amount of water in mixtures (including the water in the superplasticizer) was 141 l/m³.

The concrete was cast in 32 × 16 cm cylindrical molds, which were filled in two successive stages with a needle vibration. The specimens were stored in their molds for 24 h at a temperature of 20 ± 1°C and at a relative humidity of 55 ± 5%. They were then demoulded and cured in lime-saturated water at 20 ± 1°C until required for testing. The

TABLE 2
Mix proportions and properties of fresh concrete.

Mixture	w/(c+sf)	sf/(c+sf) (%)	Batch quantities (kg/m ³)				*SP (%)	Properties of fresh concrete		
			Cement	Silica Fume	Fine Agg.	Coarse Agg.		Slump (mm)	Unit weight (kg/m ³)	Air content (%)
C1	1	0	550	0	638	1192	5.5	160	2551	1.2
	2	0.25	495	55	640	1200	2.8	170	2546	1.5
	3	12	440	110	620	1190	3.4	160	2520	1.3
	4	30	385	165	610	1172	4	170	2495	1.1
	5	0	460	0	688	1208	2.6	180	2509	1.6
	6	0.30	414	46	682	1206	1.6	190	2496	1.7
	7	20	368	92	674	1188	2.4	170	2474	1.2
	8	30	322	138	670	1170	2.8	170	2454	0.9
	9	0	400	0	744	1196	1.4	160	2489	1.5
	10	0.35	360	40	734	1195	1	170	2476	1.4
	11	20	320	80	730	1176	1.6	170	2456	1.1
	12	30	280	120	720	1165	2	170	2437	1.6
	13	0	310	0	760	1152	0.6	170	2366	1.4
	14	0.45	279	31	754	1147	0.4	180	2354	1.3
	15	20	248	62	748	1137	0.8	170	2340	1.4
	16	30	217	93	740	1129	1	170	2326	0.9
	17	0	460	0	684	1213	1.8	190	2506	1.3
	18	0.30	414	46	680	1209	0.8	190	2494	1.5
	19	20	368	92	670	1197	1.2	170	2474	1.4
	20	30	322	138	668	1172	2	180	2450	1.1
C2	21	0	400	0	740	1202	0.6	200	2485	0.9
	22	0.35	360	40	732	1196	0.4	210	2471	1.5
	23	20	320	80	726	1183	0.8	200	2453	1.4
	24	30	280	120	714	1177	1	190	2436	0.8

*SP: Superplasticizer (water + solids), percent by weight of the cementitious materials (c+sf).

cylinders were tested in compression with a servo-hydraulic press (standard AFNOR NF 18-406). Each strength value was the average of the strength of three specimens.

Results and Discussion

Influence of Superplasticizer Dosage and Silica Fume Content on the Workability of Concretes

Figures 1 and 2 show the influence of superplasticizer dosage on the water requirement with a constant slump. The results of Figure 1 confirm the efficiency of superplasticizer as water-reducer whatever the percentage of silica fume (sf). For a 10% sf content, the superplasticizer dosage is lower than that of the control concrete. For this content, the dosage is minimum regardless of the w/(c + sf) ratio and the minimum is all the more important as the ratio is low. The results show that we can replace up to 10% cement and at the same time

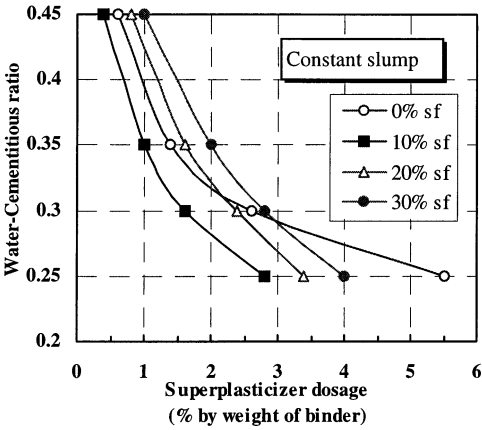


FIG. 1.
Effect of superplasticizer dosage on the water-cementitious materials ratio.

improve the workability of the concrete. Combined with the superplasticizer, the silica fume contributes to the dispersion action of flocculated cement particles. At a low water-cementitious materials ratio of 0.25, the superplasticizer dosage of sf concretes is inferior to that of reference concrete. The same conclusions were drawn by Sellevold and Yogendran in previous studies (8,12).

It is clear from the data in Figure 3 that the superplasticizer dosage is lower for cement with a small content of C_3A (C2) compared with an ordinary Portland cement (C1). The dosage doubles when the percentage of C_3A increases from 2% to 10%. Indeed the superplasticizer is adsorbed by C_3A phase for the first minutes of mixing and interferes with the early hydration of ettringite and C-S-H. But the superplasticizer adsorption depends both on the amount of C_3A and on the presence of soluble alkali sulfates. Thus the ratio of ionic

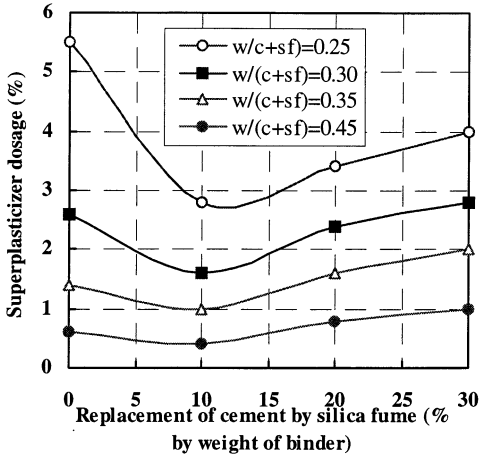


FIG. 2.
Effect of replacement of cement by silica fume on the superplasticizer dosage.

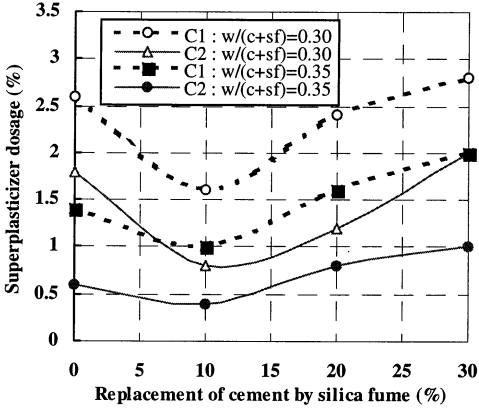


FIG. 3.
Comparison of superplasticizer dosage for the two cements.

concentration $\text{AlO}_2^-/\text{SO}_4^{2-}$, which is greater in C1 than in C2, would explain the fact that the superplasticizer adsorption varies in the same way.

We studied the evolution of slump according to time at different water-cementitious materials ratios.

With a low $w/(c + sf)$ ratio 0.25, Figure 4 shows that after a rest of 20 min., the slump loss increases quickly with time and with the content of sf. In Figure 5, for a medium $w/(c + sf)$ of 0.35, the slump loss is smaller and diminishes when the content of silica fume increases which differs from the case mentioned above.

The comparison between the curves in Figure 6 shows that the slump loss is smaller for C2 cement than for C1 cement.

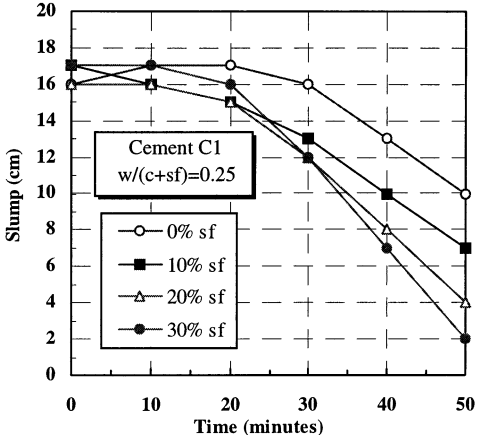


FIG. 4.
Evolution of slump loss at water-cementitious materials ratio of 0.25.

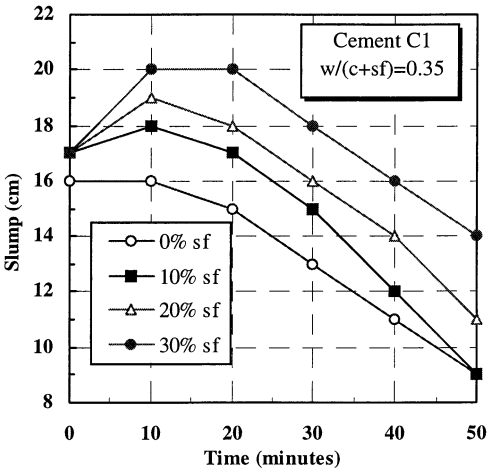


FIG. 5.

Evolution of slump loss at water-cementitious materials ratio of 0.35.

Evolution and Prediction of the Compressive Strength

The evolution of the compressive strength for different water-cementitious materials ratios between 1 day and 180 days is represented in Figure 7. It is clear from the curves of Figure 7 that the compressive strength of concrete incorporating 10 and 20% sf increases compared to the control concrete without sf. On the contrary at a level of 30% sf, the strength is slightly lower.

Between 1 (t_1) and about 10 days (t_d), the compressive strength R increases linearly according to the logarithm of time t :

$$R = A + B \log \frac{t_d}{t_1}$$

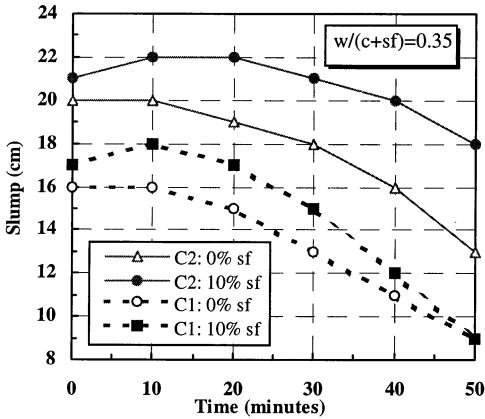


FIG. 6.

Evolution of slump loss for the two cements at water-cementitious materials ratio of 0.35.

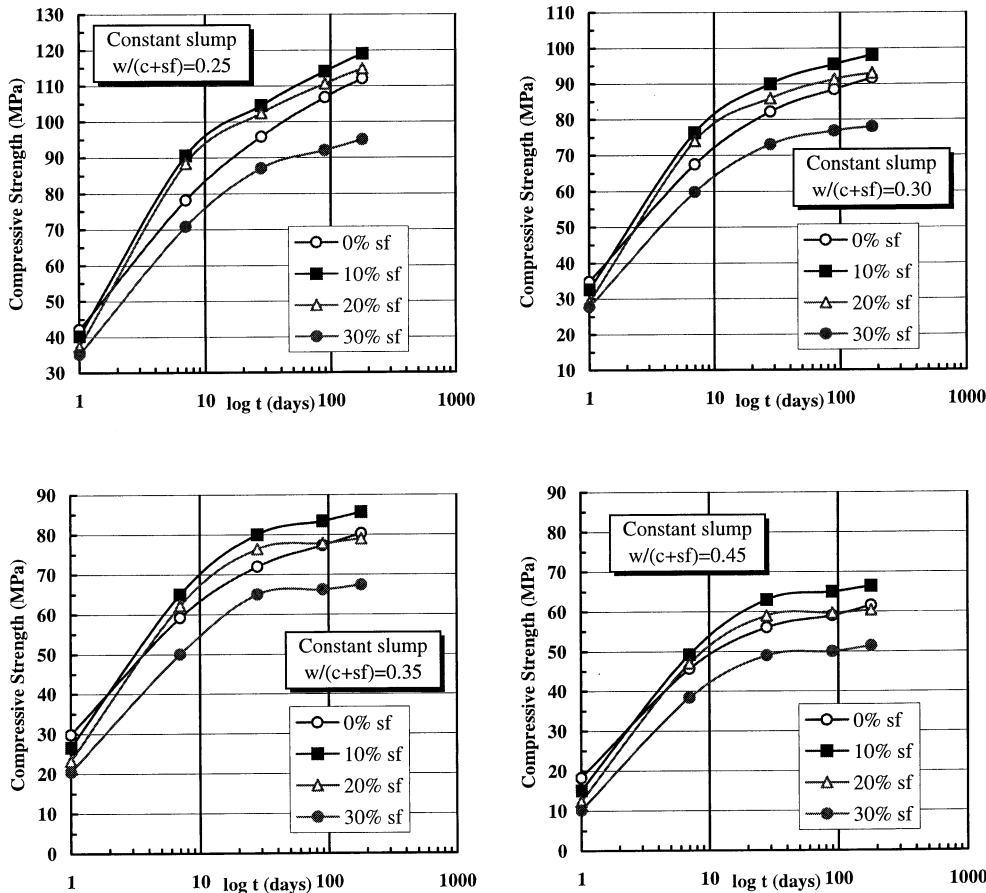


FIG. 7.

Strength development of concretes at different water-cementitious materials ratios.

The B coefficient represents the kinetics of the hydration reaction. For sf concrete the kinetics is activated by the pozzolanic effect of the silica fume which starts early before two days (13). The variation of the B/B_0 (B_0 for the control concrete) quotient as a function of $w/(c + sf)$ ratio is shown in Figure 8. It can be observed from the curves that the kinetics of the pozzolanic reaction decreases when the $w/(c + sf)$ ratio increases. It is obvious that the highest pozzolanic effect is due to 10–20% sf contents. For 30% sf, the granular dispersion of a great number of sf particles makes up for the pozzolanic effect.

After 10 days we notice a reduction regarding the kinetics of the increase in the strength of mixes, but the reduction is less important for the control concrete. In the long run, the compressive strength of the control concrete is the same as the 10% and 20% sf concretes. Figure 9 shows that the compressive strength increases normally when the $w/(c + sf)$ ratio diminishes; moreover, the influence of the water-cementitious materials ratio is more important than the incorporation of silica fume.

The variation of the ratio $R_{sf}/R(\text{control})$ as a function of the sf content after 28 and 180 days for the four investigated water-cementitious ratios is presented in Figure 10. By

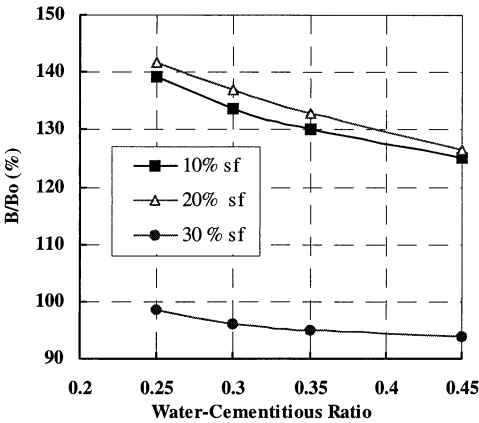


FIG. 8.

Kinetics of the pozzolanic reaction as a function of water-cementitious materials ratio.

analysing the curves, we notice that the optimum replacement of cement by sf is around 10–15% sf. This result is in agreement with the conclusions reached by other investigators (8,9). However, the percentage of the increase in compressive strength for 10% sf concretes remains quite low, about a maximum of 15% after 28 days. Furthermore, the increase tends to be less important in the long run.

Figure 11 compares the evolution of strength as a function of time for the cements C1 and C2 at a $w/(c + sf) = 0.30$. We notice that the curves have approximately the same shape and the results are similar to that of other water-cementitious materials ratios. The cement C1 that contains more C_3A than C2 has a rapid kinetics hydration in the short term, but we obtain approximately the same strength at later ages.

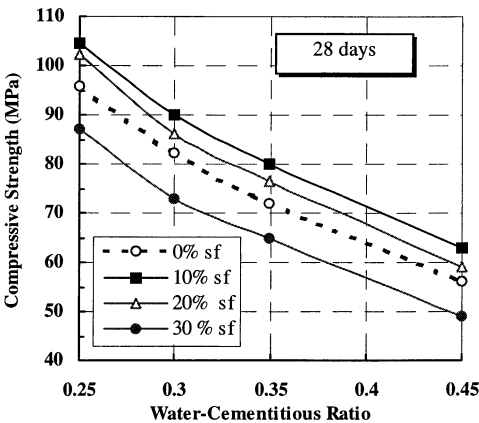


FIG. 9.

Variation of the compressive strength as a function of water-cementitious materials ratio.

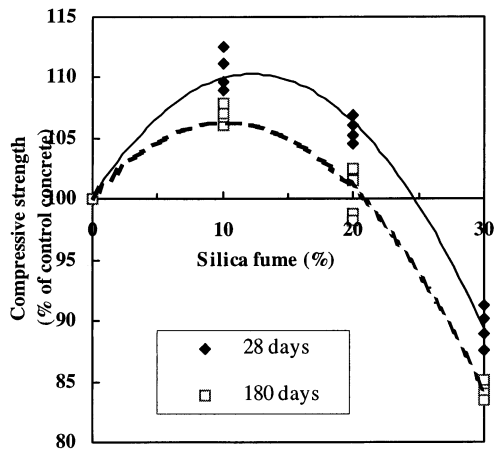


FIG. 10.

Effect of silica fume on compressive strength at different water-cementitious materials ratios.

Prediction of Strength Development of sf Concretes

The compressive strength of an ordinary concrete after 28 days may be represented by the Bolomey equation (14):

$$f_{c28} = KR_{c28} \left(\frac{C}{E + V} - 0.5 \right) \tag{1}$$

where C and E are the mass of cement and water, V is the air volume, K is a coefficient that depends on the characteristics of aggregates, and R_{c28} is the compressive strength of the standardized mortar after 28 days.

For sf concretes, we present a simple equation of the same type:

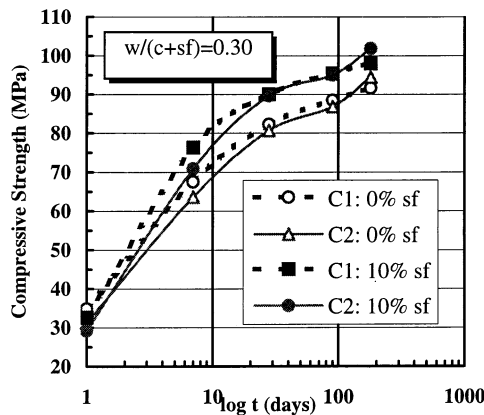


FIG. 11.

Strength development of the two cements with a water-cementitious materials ratio of 0.30.

TABLE 3
Composition and compressive strength of standardized mortar specimens $4 \times 4 \times 16$ cm (NF P15-451).

No. mixture	1	2	3	4	5	6	7
sf/c	0	0.1	0.15	0.2	0.25	0.3	0.4
w/(c+sf)	0.3	0.294	0.29	0.3	0.3	0.3	0.3
w (g)	165	150	135	132	132	120	105
c (g)	550	510	500	450	440	400	350
sf (g)	0	51	75	90	110	120	140
Sand (g)	1350	1350	1350	1350	1350	1350	1350
Superpl.(%)	1.5	1.5	2.0	2.2	2.4	2.8	3.0
f_{c28} (MPa)	83	102	109	112	114	112	108
α (sf/c)	0.005	0.196	0.261	0.341	0.364	0.340	0.292

$$f_{c28} = KR_{c28} \frac{1}{\rho_c} \frac{L}{(E + V)} \quad (2)$$

where ρ_c is the relative density of the cementitious material and L is the effective cementitious content such as $L = C + \alpha(\text{sf}/c)C$. The function $\alpha(\text{sf}/c)$ represents the contribution of sf in “equivalent” cement to the compressive strength. We may assume that the efficiency of sf is linked to the presence of cement and only depends on the sf/c ratio.

Eventually, we obtain the following equation:

$$f_{c28} = KR_{c28} \frac{1}{\rho_c} \frac{C}{(E + V)} [1 + \alpha(\text{sf}/c)] \quad (3)$$

In order to determine the $\alpha(\text{sf}/c)$ function, we measured the compressive strength on standardized mortar specimens with increasing sf contents.

The composition, the compressive strength at 28 days, and the values of the $\alpha(\text{sf}/c)$ function calculated from Eq. 3 are listed in Table 3. The curve represents the variation of the α coefficient with the sf/c ratio is shown in Figure 12. By smoothing the experimental data, the curve can be represented by the following equation obtained with a correlation coefficient of 0.989:

$$\alpha(\text{sf}/c) = 0.36 - [2.1(\text{sf}/c) - 0.6]^2$$

The air volume of Eq. 3 is taken into account by writing $V = yE$. The y coefficient depends on the concrete consistency according to the following values: 0.13 for a firm concrete, 0.10 for a plastic concrete and 0.07 for a very plastic or fluid concrete (15).

We can generalize the previous equation at any time t by writing:

$$f_c(t) = KR_{c28} \frac{C}{(y + 1) \cdot E} \{A(t) + 1.36 - [2.1(\text{sf}/c)^2 - 0.6]^2\} \quad (4)$$

The K coefficient depends on the aggregates and will be calculated from the reference concrete strength without sf at 28 days. $A(t)$ is a kinetics function that is determined from the compressive strength of reference concrete at a time t , considering that $A(t) = 0$ at 28 days.

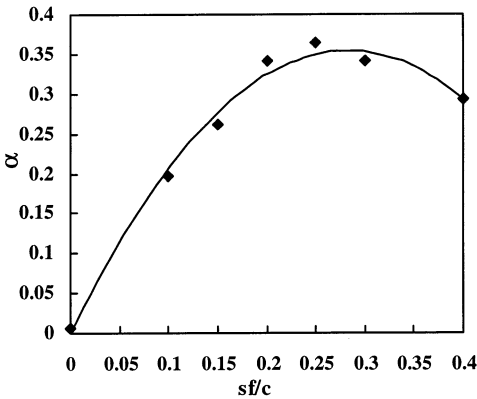


FIG. 12.
Variation of the α function with the sf/c ratio.

Figure 13 shows the results obtained by the authors and data related to the works of different researchers. All the values shown on the curve amount to 282 results (17–29). In Figure 13, the good accuracy of the model for predicting the compressive strength of sf concretes is emphasized. The absolute value of the standard deviation between the model and the experimental data is 2.9 MPa with a correlation coefficient of 0.991. The accuracy is all the more noteworthy as the model does not take into account the nature of silica fume used by the different experimenters. So the amount of SiO_2 and unburnt carbon may greatly vary according to the industrial origin of silica fume.

That model may be compared to that obtained by de Larrard (21), which is based on the Feret’s law and gives the compressive strength of sf concrete at 28 days:

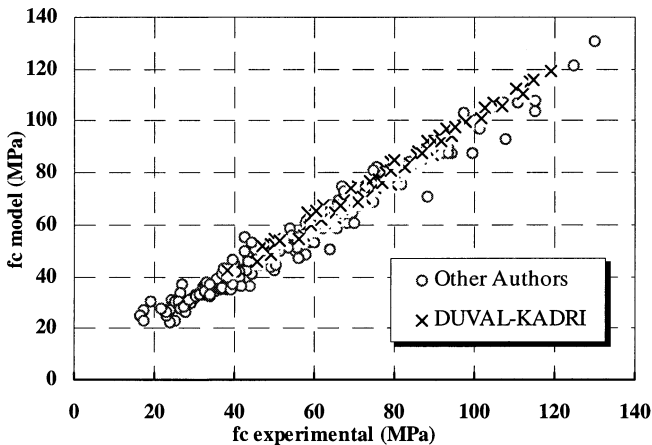


FIG. 13.
Comparison of experimental and theoretical values of the compressive strength at any time.

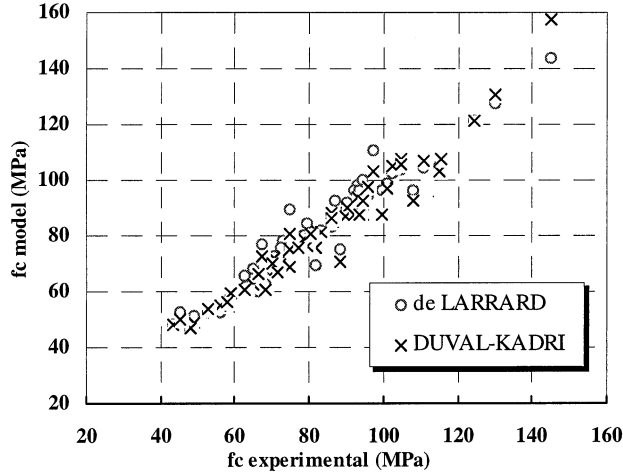


FIG. 14.

Comparison of experimental and theoretical values of the compressive strength at 28 days for the two models.

$$f_{c28} = \left[\frac{KR_{c28}}{1 + 3.1 \frac{E/C}{1.2 - 0.4 \exp(-11sf/c)}} \right]^2 \quad (5)$$

The formula is valid for water/cement ratios less than 0.40.

The comparative results from the two models are shown in Figure 14. The precision is about the same for the application of two models to the 65 experimental values obtained by the authors.

Moreover Babu and Prakash (16) evaluated the efficiency of silica fume in concrete taking into account a “percentage efficiency factor k_p ” given by the following relation:

$$k_p = 0.0015 p_r^2 - 0.1223 p_r + 2.8502$$

where p_r is the sf percentage compared with the total cementitious.

Insertion of k_p in Eq. 4 gives:

$$f_c(t) = KR_{c28} \frac{C}{(y+1)E} \left[A(t) + 1 + (0.0015 p_r^2 - 0.1223 p_r + 2.8502) \frac{sf}{c} \right] \quad (6)$$

Figure 15 shows the comparison of experimental and theoretical values calculated from the 282 data with the Eq. 6. The validation is satisfactory since the absolute value of the standard deviation between the model and the experimental data is 4.3 MPa with a correlation coefficient of 0.979.

Conclusions

We reached the following conclusions concerning sf concretes with constant slump.

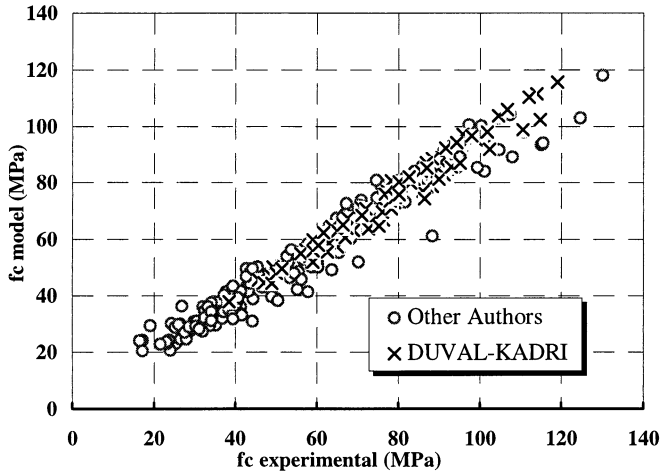


FIG. 15.

Comparison of experimental and theoretical values of the compressive strength obtained through the Eq. 6.

1. For concretes with water/cementitious materials ratios varying from 0.25 to 0.45, the superplasticizer dosage reaches a minimum for 10% sf and increases for sf contents up to 30%. Thus 10% cement may be replaced by silica fume without harming the concrete workability. Moreover, the superplasticizer dosage depends on the C_3A and alkali sulfates content of cement; it is twice as low when the C_3A content decreases from 10% to 2%.
2. The slump loss of sf concretes increases according to the percentage of silica fume for low water-cementitious materials ratios of 0.25. For higher ratios (0.35), the loss is less important and decreases with the sf content.
3. The increase of the compressive strength of sf concretes depends much more on the decrease of the water/cementitious materials ratio than on the replacement of silica fume with cement. The compressive strength increases with the silica fume content up to 20% and reaches a maximum for a 10 to 15% sf level. However the gain in strength compared with reference concrete remains less than 15%.
4. Consequently we suggest a model which enables to assess the compressive strength at a given time for sf concretes. After determining the strength of standardized mortar, values of compressive strength are obtained with a correlation coefficient 0.991 thanks to 282 experimental data based on the authors' experiments and other investigations.

References

1. A. Goldman and A. Bentur, ACI J. Mater. 86, 440 (1989).
2. C.-Y. Huang and R.F. Feldman, Cem. Concr. Res. 15, 285 (1985).
3. S.L. Sarkar and P.C. Aïtcin, Cem. Concr. Res. 17, 591 (1987).
4. J.A. Larbi, Microstructure of the Interfacial Zone Around Aggregate Particles in Concrete, 38, Heron, Delft, the Netherlands, 1993.
5. H.A. Toutanji and T. El-Korchi, Cem. Concr. Res. 25, 1591 (1995).
6. X. Cong, S. Cong, D. Darwin, and S. McCable, ACI J. Mater. 89, 375 (1992).

7. S. Popovics, *Mater. Struct. RILEM* 20, 32 (1987).
8. V. Yogendran, B.W. Langan, M.N. Haque, and M.A. Ward, *ACI J. Mater.* 84, 124 (1987).
9. M.N. Sautsos and P.L.J. Domone, *Strength Development of Low Water-Binder Ratio Mixes Incorporating Mineral Admixtures. Vol. II*, pp. 945–952, 1993.
10. V.M. Malhotra and G.G. Carette, *Concr. Int. Design Constr.* 5, 40 (1983).
11. F. de Larrard, *Cem. Concr. Aggr. ASTM* 12, 1, (1990).
12. E.J. Sellevold and F.F. Radjy, *Condensed Silica Fume (Microsilica) in Concrete: Water Demand and Strength Development. Fly-Ash, Silica Fume, Slag and Other Mineral By-Products in Concrete*, ACI SP-79, 677 (1983).
13. J.P. Ollivier, A. Carles-Gibergues, and B. Hanna, *Cem. Concr. Res.* 18, 438 (1988).
14. J. Bolomey, *Travaux*, 19, 228 (1935).
15. P.C. Aïtcin, J. Baron, and J.P. Bournazel, *Viser une Résistance à la Compression, dans les Bétons, Bases et Données pour leur Formulation*, p. 294, Eyrolles (Editeur), Paris, 1996.
16. K.G. Babu and P.V.S. Prakash, *Cem. Concr. Res.* 25, 1273 (1995).
17. P.C. Aïtcin, *Concr. Int.* October 69–72 (1988).
18. H.H. Bache, *Densified cement ultrafine particle-based materials. The Second International Conference on Super-plasticizer in Concrete*, pp. 185–213, Ottawa, June (1981).
19. C. Bedard, G. Ballivy, and P.C. Aïtcin, *Rôle des caractéristiques physico-mécaniques des granulats sur la résistance en compression des bétons à très hautes résistances. Bulletin de l'Association Internationale de Géologie de l'Ingénieur*, no. 30, Paris (1984).
20. G.G. Carette and V.M. Malhotra, *Long-term strength development of silica fume concrete. CANMET/ACI, Fly, Silica Fume, Slag and Natural Pozzolans in Concrete*, ACI SP132–55, Vol. II, pp. 1017–1044 (1992).
21. F. de Larrard, *Prévision des résistances en compression des bétons à hautes performances aux fumées de silice ou une nouvelle jeunesse pour la loi de Férret. Annales de l'ITBTP*, no. 483, mai (1990).
22. J. Djellouli, P.C. Aïtcin, and O. Chaallal, *Use of ground slag in high-performance concrete. High-Strength Concrete*, ACI SP121–18, Vol. II, pp. 351–368 (1990).
23. R. Le Roy, *Déformations instantanées et différées des bétons à hautes performances. Thèse de doctorat de l'Ecole Nationale des Ponts et Chaussées*, Paris, septembre (1995).
24. V.E. Sorensen, *Freezing and thawing resistance of condensed silica fume (Microsilica) concrete exposed to deicing chemicals. CANMET/ACI Fly, Silica Fume, Slag and Natural Pozzolans in Concrete*, SP79–37, Vol. II, pp. 709–718 (1983).
25. V.M. Malhotra, *Mechanical properties and freezing-and-thawing resistance of non-air-entrained and air-entrained condensed silica-fume concrete using ASTM test C 666 procedures A and B. CANMET/ACI, Fly, Silica Fume, Slag and Natural Pozzolans in Concrete*, SP91–53, Vol. II, pp. 1069–1094 (1986).
26. S. Seki and M. Morimoto, *Recherche expérimentale sur l'amélioration du béton par l'incorporation de sous-produits industriels. Annales de l'ITBTP*, no. 436, juillet-août (1985).
27. L.S. Marusin, *Chloride ion penetration in conventional and concrete containing condensed silica fume. Fly, Silica Fume, Slag and Natural Pozzolans in Concrete*, ACI SP 91-55, Vol. II, pp. 1119–1133 (1986).
28. O. Skjolsvold, *Carbonation depths of concrete with and without condensed silica fume. CANMET/ACI, Fly, Silica Fume, Slag and Natural Pozzolans in Concrete*, ACI SP 91-51, Vol. II, pp. 1031–1048 (1986).
29. J. Wolsiefer, *Ultra high-strength placeable concrete in the range 10.000 to 18.000 psi (69 to 124 MPa). ACI Annual Convention, Atlanta, January (1982).*